

Polydopamine-Modified Metal–Organic Framework Membrane with Enhanced Selectivity for Carbon Capture

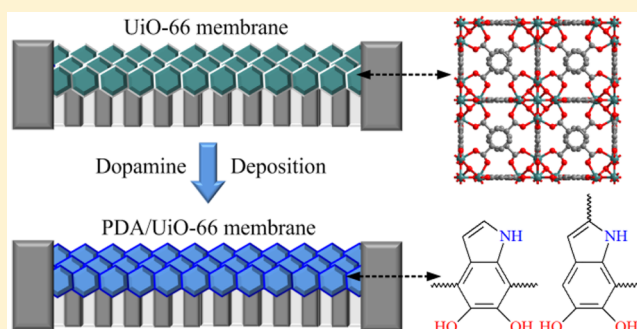
Wufeng Wu,[†] Zhanjun Li,[†] Yu Chen,[‡] and Wanbin Li^{*,†}

[†]School of Environment, and Guangdong Key Laboratory of Environmental Pollution and Health, Jinan University, Guangzhou 511443, P.R. China

[‡]Huizhou Research Institute, Sun Yat-sen University, Huizhou 516081, P.R. China

S Supporting Information

ABSTRACT: In this work, a versatile postmodification strategy based polydopamine (PDA) grafting is reported for improving CO₂ separation performance of MOF membranes. Owing to the strong bioadhesion, PDA can be deposited on the UiO-66 membrane through a simple and mild process. Since PDA impregnation in invalid nanometer-sized pinholes and grain boundaries of the MOF membrane suppress nonselective gas transports, the modified PDA/UiO-66 membrane exhibits significantly enhanced CO₂/N₂ and CO₂/CH₄ selectivities of 51.6 and 28.9, respectively, which are 2–3 times higher than the reported MOF membranes with similar permeance. Meanwhile, because PDA modification do not change UiO-66 intrinsic pores and membrane thickness is submicrometer-sized, the CO₂ permeance is 2–3 orders of magnitude larger than those membranes with similar selectivity, up to $3.7 \times 10^{-7} \text{ mol m}^{-2} \text{ s}^{-1} \text{ Pa}^{-1}$ (1115 GPU). Moreover, the PDA/UiO-66 membrane with good reproducibility has excellent long-term stability for CO₂ capture under moist condition in 36 h measurement period.



The excess emissions of greenhouse gases cause various environmental issues including global warming, ocean acidification and ecological damage.¹ With population growth and industrial progress, the atmospheric concentrations of greenhouse gases, especially carbon dioxide, are continuing to increase.^{2–5} In 2015, the atmospheric CO₂ concentration was 400 ppm, which is remarkably greater than the preindustrial level of 280 ppm.^{3–5} A package of programs to reduce CO₂ concentration, such as the Paris Agreement, have been prompted by governments and industries.^{5,6} Besides development of clean energy that can be utilized without carbon emission, capture of CO₂ from low-grade natural gases and flue gases produced by combustion of fossil/carbonaceous fuels is very important. Conventional technologies for CO₂ capture based on gas–liquid phase change, such as absorption, cryogenic distillation and condensation, are energy intensive and uneconomic.^{5–9} Membrane separation has great potential for capture of CO₂, due to its merits of simple operation, small footprint, high efficiency, no phase change and environmental friendliness.^{5,7,8,10} For membrane materials, polymeric membranes have advantages of low cost, high processability and acceptable selectivity. However, small permeability, a few tens of Barrers (1 Barrer = $3.348 \times 10^{-16} \text{ m mol m}^{-2} \text{ s}^{-1} \text{ Pa}^{-1}$), brings about a stringent requirement of large membrane area, even for dealing with a small industrial station, which increase equipment costs tremendously.^{11,12} In order to improve permeation property, inorganic micro/nanoparticles are used

as fillers for changing the formation and construction of polymeric membranes to form mixed-matrix membranes (MMMs).^{13–16} Some other materials, for example, zeolites, metal–organic frameworks (MOFs), microporous polymers, and graphene and its derivatives, have been proposed for fabricating high-performance membranes as well.^{11,17–22}

Thanks to the large surface areas, appropriate apertures and unique affinities, MOF membranes show impressive performance in hydrogen purification and hydrocarbon separation, and can easily surpass the trade-off line of polymeric membranes.^{23–26} For examples, the CuBTC membranes exhibited high permeance and H₂/CO₂ selectivity about 7–10,^{27,28} the NH₂-MIL-53 membranes could separate H₂/CO₂, H₂/N₂ and H₂/CH₄ mixtures with selectivities about 20–30,^{29,30} and the ZIF-8 membranes displayed excellent propylene permselectivity over propane.^{31–34} Comparatively, the reports about MOF membranes for CO₂ capture are relatively fewer. Yin et al. reported that the amino-functionalized CAU-1 membrane had high CO₂ permeance of $8.0 \times 10^{-7} \text{ mol m}^{-2} \text{ s}^{-1} \text{ Pa}^{-1}$ and CO₂/N₂ selectivity of 14.8.³⁵ Cacho-Bailo et al. deposited the ZIF membranes on inner surface of polymeric hollow fibers. The membranes showed CO₂/CH₄ selectivity up to 37.7,

Received: January 19, 2019

Revised: March 3, 2019

Accepted: March 5, 2019

Published: March 5, 2019

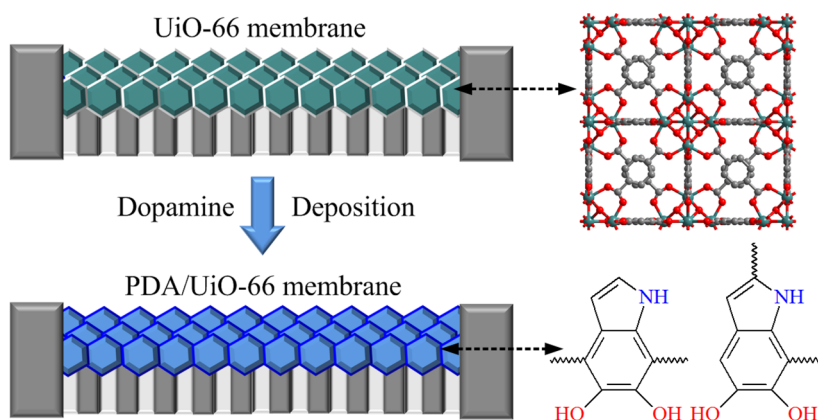


Figure 1. Schematic for postmodification of the UiO-66 membrane by PDA.

while small permeance about $1.2 \times 10^{-9} \text{ mol m}^{-2} \text{ s}^{-1} \text{ Pa}^{-1}$.^{36,37} From the economic evaluation, the membranes with high permeance over 1000 GPU ($1 \text{ GPU} = 3.348 \times 10^{-10} \text{ mol m}^{-2} \text{ s}^{-1} \text{ Pa}^{-1}$) and good selectivity larger than 20 are desired for CO_2 capture from flue gases.^{12,38} Therefore, the CO_2 separation performance of MOF membranes should be improved further.

Postmodification is commonly applied for adjusting the pore structures and adsorptions of MOF materials.³⁹ For MOF membranes, molecular sieving is a well-known mechanism for gas separation. However, precise design of MOFs with pore size between the kinetic diameters (KD) of two light gases, such as CO_2 (KD: 0.33 nm) and N_2 (KD: 0.364 nm), is extremely difficult. Moreover, the flexibility of frameworks increases the difficulty of structural construction. The interaction between MOFs and components to be separated significantly influences performance as well.⁴⁰ On the one hand, superior affinity of penetrated component in MOFs may enhance its sorption or diminish the diffusion of blocked component, and then improve selectivity. On the other hand, strong interaction of blocked molecules in MOFs may suppress molecule migration in membranes, thereby leading to high permselectivity. In addition to regulation of apertures and affinities, postmodification can restrain the bypass gas penetration through the noneffective nanometer-sized pinholes and grain boundaries, and then enhance separation performance.^{41–45} Huang et al. modified the ZIF-90 membranes by ethanolamine and 3-aminopropyltriethoxysilane.^{41,44} The grafted MOF membranes with constricted pore sizes and reduced nonselective passageways showed improved H_2 permselectivity. To increase the permeance of MOF membranes, Lee et al. employed linker exchange for transforming the top layer of the ZIF-8 membrane to ZIF-90 that had larger apertures.⁴⁵ However, the modification based on the reaction between the introduced substances and linkers with functional groups limits the types of applied MOFs. Herein, we report a versatile polydopamine (PDA) postmodification strategy to obtain high-performance MOF membranes for CO_2 capture, because PDA can be simply deposited on membranes owing to its strong bioadhesion.^{46–48}

EXPERIMENTAL DETAILS

Materials. ZrCl_4 , 1,4-dicarboxybenzene (BDC), *N,N*-dimethylformamide (DMF) and methanol were purchased from Kutai Chemical Reagent Co., China. Anodic alumina oxide (AAO) substrate with pore size of 20 nm and diameter

of 25 mm was supplied by Liangwen Chemical Reagent Co., China. All reagents were used as received.

Preparation of UiO-66 Membranes. ZrCl_4 (0.16 g), BDC (0.11 g) and deionized water ($11.9 \mu\text{L}$) were dispersed in DMF (25 mL). The mixture was dissolved by ultrasonic treatment to obtain transparent solution. For seeding, AAO substrate was horizontally immersed in precursor solution and thermally treated at $120 \text{ }^\circ\text{C}$ for 3 days. After natural cooling, the AAO substrate covered with UiO-66 crystals was taken out and tenderly washed by DMF. For preparation of the UiO-66 membrane, the seeded AAO substrate was vertically soaked in precursor solution and treated under the same conditions as seeding for another two times. After crystallization, the prepared UiO-66 membrane was washed by DMF and methanol, and then dried at room temperature for use.

Preparation of PDA/UiO-66 Membranes. 3-Hydroxytyramine hydrochloride (40 mg) was dissolved in deionized water (20 mL). To make the dopamine enter into the potential pinholes of membranes as much as possible, the prepared UiO-66 membrane was first soaked in above solution at room temperature for 12 h. The dopamine buffering solution with pH of 8.5 was prepared adding tris(hydroxymethyl)aminomethane (THAM) solution (24 mg THAM in 20 mL water) in 3-hydroxytyramine hydrochloride solution. For PDA postmodification, the UiO-66 membrane after soaking was immersed in buffering solution for another 12 h. After deposition, the white UiO-66 membrane changed to the dark brown PDA/UiO-66 membrane. The prepared PDA/UiO-66 membrane was washed by deionized water to remove the unreacted dopamine, and then dried at room temperature.

Separation Performance. The experimental setup for gas permeation and separation is presented in [Supporting Information \(SI\) Figure S1](#). The membrane with exposed area of 2.5 cm^2 was sealed in a permeation cell by O-ring. The chamber with exposed MOF layer was applied as feed side. The permeation data was recorded after running steadily. For single-gas permeation, various gases were measured with order of H_2 , CO_2 , N_2 , CH_4 , CH_4 , N_2 , CO_2 , and H_2 . The ideal selectivity ($\alpha_{i/j}$) was calculated as the ratio of two gas permeances (P) by $\alpha_{i/j} = P_i/P_j$. For gas separation, the binary mixture of CO_2/N_2 or CO_2/CH_4 was used as feed gases with flow rate of 50 mL min^{-1} . The temperature was kept at $25 \text{ }^\circ\text{C}$. The sweep gas was Ar with flow rate of 50 mL min^{-1} . The feed pressure was 0.1 MPa. The gas concentration was studied by using a gas chromatography (GC-6890), which was equipped with a thermal conductivity detector (TCD) and a steel

column (TDX-01). The temperatures of column, vaporization chamber and TCD were 80, 150, and 150 °C, respectively. The mixture selectivity ($\alpha_{i/j}$), for example of CO₂/N₂ separation, was calculated through dividing the ratio (i -CO₂ to j -N₂) of the permeate mixture y_i/y_j by the ratio (i -CO₂ to j -N₂) of the retentate mixture x_i/x_j , $\alpha_{i/j} = (y_i/y_j)/(x_i/x_j)$.

Characterizations. The crystalline structure of the samples was investigated by X-ray diffraction (XRD) (D2 Phaser, Bruker CO.) with Cu K α radiation at 30 kV and 10 mA. The sample was scanned between 5° and 40° with step size of 0.01° and scan speed of 0.2 s per step. The morphology of the membranes was characterized by using a field-emission scanning electron microscope (SEM) (Ultra-55, Zeiss Co.). The chemical structure of the samples was studied by using a Fourier transform infrared spectrophotometer (FT-IR, IRTracer-100, Shimadzu CO.). A RBD upgraded PHI-5000C ESCA system (PerkinElmer) was employed to perform X-ray photoelectron spectroscopy (XPS) experiment. Gas adsorption and desorption isotherms were recorded by using a physisorption analyzer (Autosorb iQ, Quantachrome Co.). The specific surface area was calculated by Brunauer–Emmett–Teller (BET) method. Gas adsorption isotherms were collected at temperature of 25 °C.

RESULTS AND DISCUSSION

Preparation of UiO-66 Membranes. The postmodification of MOF membranes is presented in Figure 1. As above-mentioned, the strong differentiation in affinity of MOFs to feed components may be beneficial to membrane separation. UiO-66,⁴⁹ a chemically stable Zr-MOF with octahedral cage, is composed of Zr₆O₄(OH)₄ nodes and BDC linkers. Because of the large adsorption capacity for CO₂,^{50–52} UiO-66 was employed as probe for synthesizing MOF membranes. For seed deposition, AAO substrate was horizontally immersed in precursor solution and thermally treated at 120 °C for 3 days. To obtain the UiO-66 membrane, the seeded substrate was vertically in precursor solution and treated under the same conditions for another two times. The obvious characteristic peaks in XRD pattern of the prepared membrane indicated that the synthesized layer had pure UiO-66 crystalline structure (Figure 2). For MOF membrane synthesis, the heterogeneous growth on substrates is beneficial to formation of continuous membranes, yet the competition from homogeneous crystallization in solutions is undesirable.⁵³ Because there no

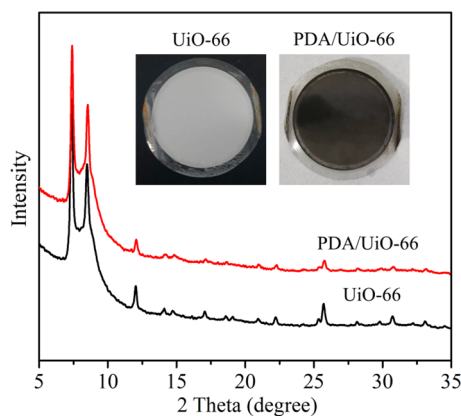


Figure 2. Photographs and XRD patterns of the UiO-66 and PDA/UiO-66 membranes.

sufficient heterogeneous nucleation sites existed on substrates, the substrate after first thermal treatment for seeding was covered with an uncontinuous UiO-66 layer (SI Figure S2a). After synthesis for three times, since the uncontinuous UiO-66 layer improved the heterogeneous crystallization as seeds, an intergrown UiO-66 membrane was obtained, which could be observed from the cross-sectional view SEM image (Figure 3a). The thin UiO-66 membrane had thickness of $\sim 0.8 \mu\text{m}$,

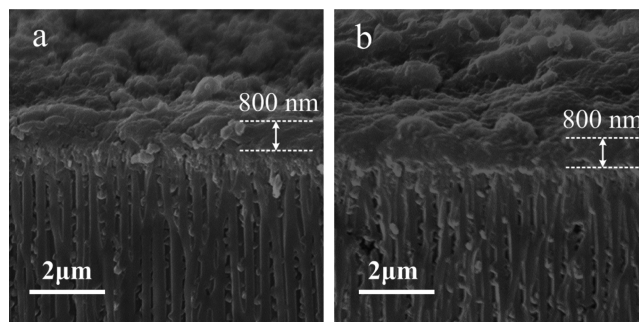


Figure 3. SEM images of (a) the UiO-66 membrane and (b) the PDA/UiO-66 membranes.

which was smaller than that of most reported MOF membranes.^{19,24} SEM image with low magnification indicated that the prepared UiO-66 membrane was uniform in large scale (SI Figure S2). Besides AAO substrate, polymeric hollow fibers with high processability, low cost and large membrane area per volume could also be employed to prepare the UiO-66 membranes (SI Figure S3).

Post-Modification of UiO-66 Membranes. For post-modification, the prepared UiO-66 membrane was first immersed in dopamine aqueous solution to make the introduced component enter into the potential pinholes as much as possible. The UiO-66 membrane with impregnated solution was transferred in dopamine buffering solution (pH 8.5) and maintained at room temperature for 12 h. Dopamine could spontaneously polymerized into PDA and deposited on membrane surface. After modification, the color of the UiO-66 membrane transferred from white to dark brown (Figure 2, inset), suggesting the successful PDA deposition.⁵⁴ Because of the excellent water stability of UiO-66,⁴⁹ the PDA/UiO-66 membrane maintained good crystalline structure after modification (Figure 2). As shown in SEM image (Figure 3b), the modified membrane was still continuous. The membrane thickness showed almost no change relative to the original one, because the PDA layer was ultrathin. Unlike the post-modification of MOF membranes in previous studies,^{41,44} which would destroy the structure of frameworks more or less, benefited from the mild conditions of modification and excellent stability of UiO-66, the PDA postmodification did not impact MOF membrane structures.

To confirm the PDA modification, we investigated the chemical structures of the UiO-66 and PDA/UiO-66 membranes. As shown in Figure 4a, C 1s XPS spectrum of the UiO-66 membrane presented intensive peaks of C—C/C—H at 284.5 eV, C—COOH at 285.2 eV and O—C=O at 288.4 eV,⁵⁵ which were consistent with the chemical structure of BDC linkers. After PDA modification, a new characteristic peak at 285.8 eV for C—N, C=N and C—OH occurred (Figure 4b). This result proved that the PDA layer was formed on the surface of the UiO-66 membrane. The strong nitrogen

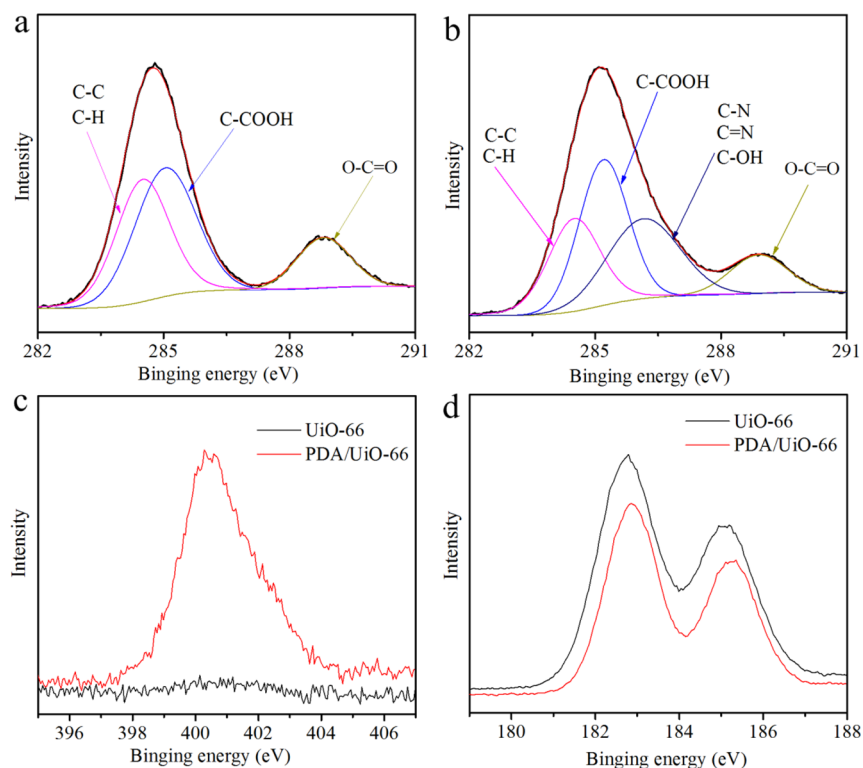


Figure 4. High-resolution C 1s XPS spectra of (a) the UiO-66 membrane and (b) the PDA/UiO-66 membrane. High-resolution (c) N 1s and (d) Zr 3d XPS spectra of the UiO-66 membrane and the PDA/UiO-66 membrane.

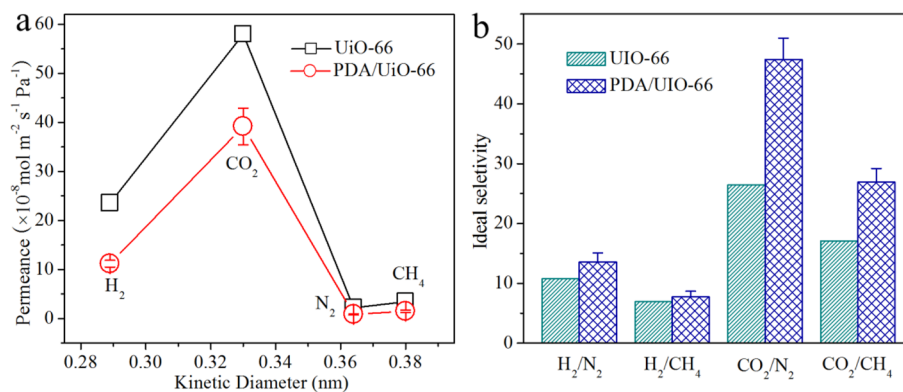


Figure 5. (a) Gas permeation properties and (b) the ideal selectivities of various gases through the UiO-66 and PDA/UiO-66 membranes.

peak in spectrum of the PDA/UiO-66 membrane testified the presence of PDA on modified membrane again (Figure 4c). The spectra of both two membranes displayed Zr 3d peaks, while the peak intensity of the PDA/UiO-66 membrane was smaller than that of the original one due to PDA coating (Figure 4d). The Zr 3d peak in spectrum of the modified membrane implied that the PDA layer was ultrathin, on account of the small XPS detecting depth of several nanometers.⁵⁶ The deposition of PDA was also analyzed by FTIR (SI Figure S4). Both UiO-66 and PDA/UiO-66 membranes exhibited the peaks at 660 cm^{-1} for stretching vibration of O–Zr bond and at 1585 cm^{-1} for asymmetric stretching vibration of O–C–O bond.⁵⁷ Two new characteristic peaks of PDA at 1270 and 1492 cm^{-1} appeared in the spectrum of the modified UiO-66 membrane. These peaks were derived from the stretching vibration of C–O–NH₂ bonds and bending vibration of N–H bond.⁵⁸ All XPS and

FT–IR results demonstrated the successful self-polymerization of dopamine on the surface of the UiO-66 membrane.

Separation Performance of UiO-66 and PDA/UiO-66 Membranes. The single-gas permeation properties of various gases through the UiO-66 and PDA/UiO-66 membranes were measured. Unlike the MOF membranes based on molecular sieving effect, which generally showed smaller permeances for the gases with larger kinetic diameters,^{26,41,44} the UiO-66 membrane showed higher CO₂ permeance of $5.8 \times 10^{-7} \text{ mol m}^{-2} \text{ s}^{-1} \text{ Pa}^{-1}$ than that of H₂ (KD: 0.289 nm), N₂ and CH₄ (KD: 0.38 nm) (Figure 5a). This phenomenon was explained by that the UiO-66 membrane was mainly governed by preferential adsorption. In other words, although the H₂ might have faster diffusion rate than CO₂, its lower adsorption led to the smaller permeance. The ideal selectivities of H₂/N₂, H₂/CH₄, CO₂/N₂ and CO₂/CH₄ were 10.8, 6.9, 26.5, and 17.0, respectively (Figure 5b), which were obviously greater than the corresponding Knudsen diffusion coefficients and similar to

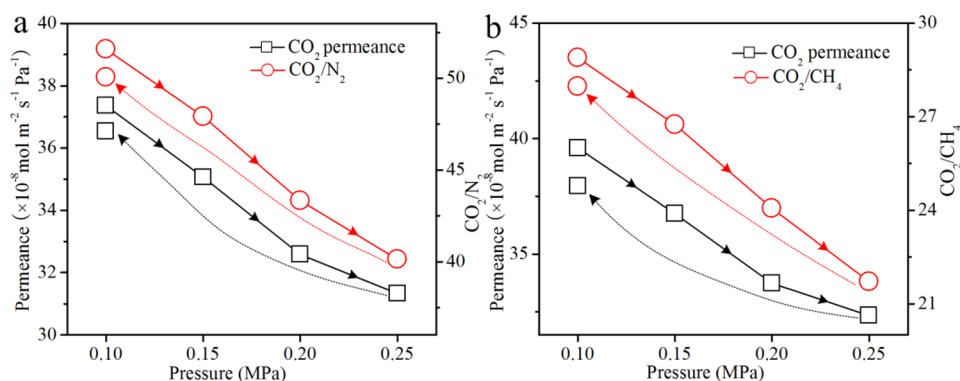


Figure 6. Gas separation performance of the PDA/UiO-66 membrane for CO_2/N_2 and CO_2/CH_4 binary mixtures under various pressures.

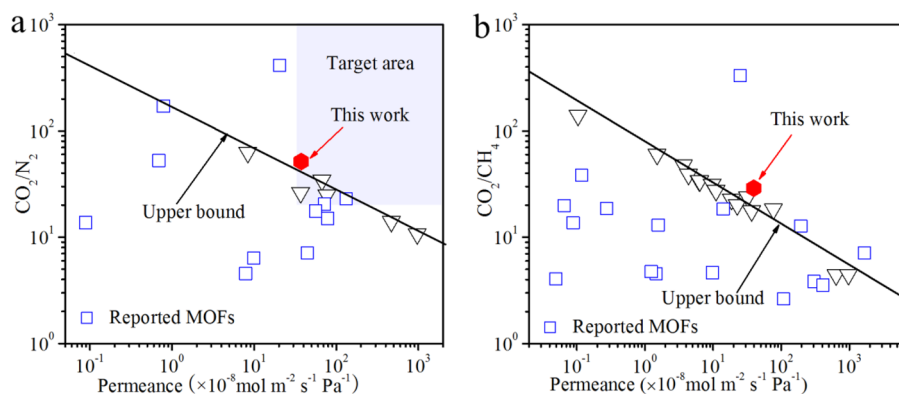


Figure 7. Comparison of the PDA/UiO-66 membrane with polymeric and other MOF membranes for (a) CO_2/N_2 and (b) CO_2/CH_4 separations. Triangles and squares represent the separation performance of polymeric and reported MOF membranes, respectively. Target area represents permeance over 1000 GPU (equal to $3.35 \times 10^{-7} \text{ mol m}^{-2} \text{ s}^{-1} \text{ Pa}^{-1}$) and selectivity over 20. The data are shown in SI Tables S4 and S5. For calculating the permeance, the thickness of polymeric membrane was assumed as $1.0 \mu\text{m}$.

those reported in previous study.⁵⁹ After postmodification, CO_2 permeance decreased as expected, but still kept at $3.9 \times 10^{-7} \text{ mol m}^{-2} \text{ s}^{-1} \text{ Pa}^{-1}$ (Figure 5a and SI Table S1). Compared with the MOF membranes modified by the reaction between linkers and grafting molecules,⁴¹ which showed great reduction in permeance, PDA modification impacted the permeation tenderly, because the framework maintained the intact interior pore structures. Furthermore, the ideal selectivities increased substantially, and reached at 13.6 (H_2/N_2), 7.7 (H_2/CH_4), 47.4 (CO_2/N_2), and 26.9 (CO_2/CH_4) (Figure 5b and SI Table S1). The effect of PDA modification procedures on gas permeation was assessed. The excess PDA deposition caused permeance decrease, while the less deposition influenced the enhancement in selectivity (SI Table S2).

We evaluated the separation performance of the PDA/UiO-66 membrane (M1) by capturing CO_2 from N_2 and CH_4 . CO_2/N_2 and CO_2/CH_4 binary mixtures with CO_2 concentration of 50% were employed as feed gases. Compared with the single-gas permeation, the CO_2 permeance at 0.1 MPa slightly decreased to $3.7 \times 10^{-7} \text{ mol m}^{-2} \text{ s}^{-1} \text{ Pa}^{-1}$ for separation of CO_2/N_2 mixture, while the CO_2/N_2 selectivity even raised to 51.6. These were interpreted by the adsorption competition between two feed gases toward the selective layer. The effect of pressure on separation performance is presented in Figure 6. For CO_2/N_2 mixture, when the pressure was up to 0.25 MPa, the CO_2 permeance and CO_2/N_2 selectivity reduced to $3.1 \times 10^{-7} \text{ mol m}^{-2} \text{ s}^{-1} \text{ Pa}^{-1}$ and 40.1, respectively (Figure 6a). The reductions of permeance and selectivity were attributed to that the enhanced entrance of N_2 in frameworks

under high pressure caused more competition for transport channels, and larger gas fluxes through the MOF membrane under high pressure led to more serious concentration polarization.^{26,28,40} For CO_2/CH_4 separation, the similar phenomena were observed (Figure 6b). The PDA/UiO-66 membrane exhibited CO_2 permeance of $3.9 \times 10^{-7} \text{ mol m}^{-2} \text{ s}^{-1} \text{ Pa}^{-1}$ and CO_2/CH_4 selectivity of 28.9 at 0.1 MPa. With the increasing of pressure, the permeance and selectivity decreased to $3.2 \times 10^{-7} \text{ mol m}^{-2} \text{ s}^{-1} \text{ Pa}^{-1}$ and 21.7, respectively. When the pressure returned to pressure of 0.1 MPa, the permeance and selectivities recovered to initial ones, demonstrating the good pressure stability of the PDA/UiO-66 membrane. The effect of the CO_2 concentration of feed mixtures on separation performance of the PDA/UiO-66 membrane was investigated. The selectivity and permeance increased as CO_2 concentration increased (SI Figure S5). It should be noted, for the CO_2 concentration of 10%, atypical CO_2 concentration in flue gas, the selectivity and permeance still kept at 41.0 and $2.6 \times 10^{-7} \text{ mol m}^{-2} \text{ s}^{-1} \text{ Pa}^{-1}$. Long-term stability of separation membranes is important for industrial application. In a 36-h measurement period, both selectivity and permeance for CO_2/N_2 binary mixture with concentration of 50% only showed small fluctuations (SI Figure S6). Because the flue gas usually has CO_2 concentration of 10–15% and contains moisture, the long-term stability of the PDA/UiO-66 membrane for binary mixture with CO_2 concentration of 10% was evaluated under moist condition. The membrane showed stable separation performance as well (SI Figure S6). These results suggested the excellent durability of the PDA/UiO-66 membrane. For

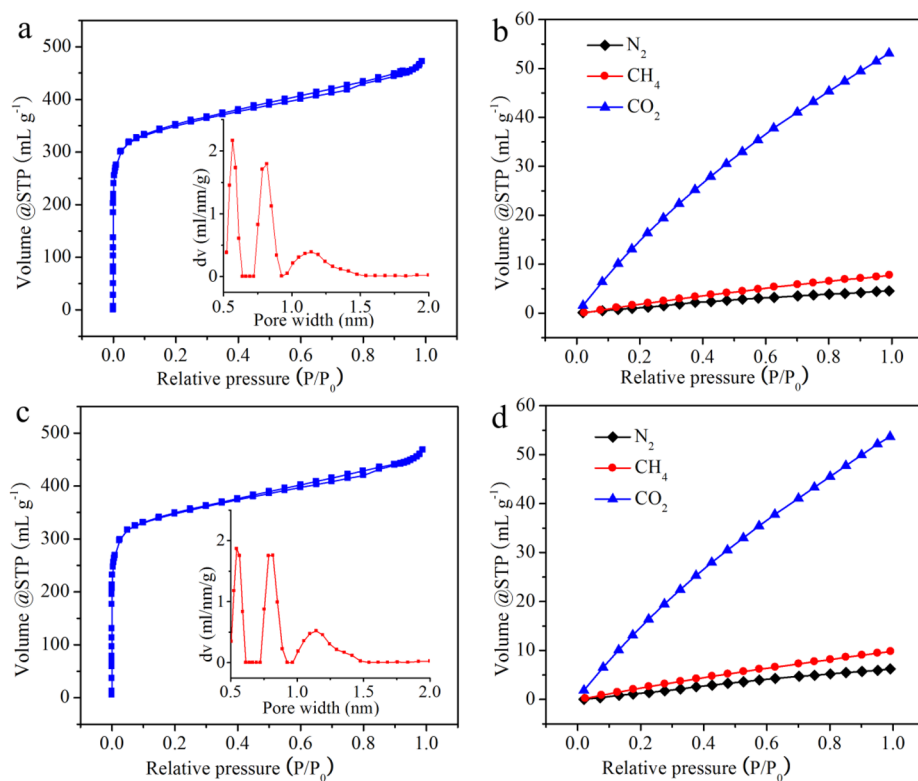


Figure 8. Nitrogen adsorption–desorption isotherms, pore width distributions and gas adsorption isotherms of (a,b) the UiO-66 and (c,d) PDA/UiO-66 particles.

studying the reproducibility, two additional membranes were prepared and employed for gas permeation and separation. The similar gas permeances and selectivities with small standard deviations indicated the good reproducibility of the PDA/UiO-66 membrane (SI Tables S1 and S3).

Comparison of Separation Performance. Figure 7 presents the comparison of CO₂ capture performance between the previously reported membranes made by polymers and MOFs, and the PDA/UiO-66 membrane in this study. The upper bound relationships between permeance and selectivity of polymeric membranes summarized by Robeson in 2008 are common standards for measuring separation performance.²³ For polymeric membranes, although the appropriate selectivity can be achieved in CO₂/N₂ and CO₂/CH₄ separations, the permeance is usually small. Obviously, the performance of the PDA/UiO-66 membrane could exceed the Robeson's upper-bound for both CO₂/N₂ and CO₂/CH₄ systems, and located in the target area (permeance >1000 GPU equal to $3.35 \times 10^{-7} \text{ mol m}^{-2} \text{ s}^{-1} \text{ Pa}^{-1}$ and selectivity >20) of CO₂ capture from flue gases for economically industrial application.^{12,38} In the field of MOF membranes for CO₂ capture, Venna and Carreon reported a ZIF-8 membrane with unprecedented high CO₂ permeance of $2.4 \times 10^{-5} \text{ mol m}^{-2} \text{ s}^{-1} \text{ Pa}^{-1}$ but low CO₂/CH₄ selectivity of 5.1.⁶⁰ Yang et al. synthesized a continuous CAU-1 membrane, which showed CO₂ permeance of $7.3 \times 10^{-7} \text{ mol m}^{-2} \text{ s}^{-1} \text{ Pa}^{-1}$ and CO₂/N₂ selectivity of 20.3.⁶¹ Caro et al. fabricated a ZIF-8 membrane by conversion of ZnAl-NO₃ layered double hydroxide. The obtained membrane displayed CO₂ permeance of $1.6 \times 10^{-8} \text{ mol m}^{-2} \text{ s}^{-1} \text{ Pa}^{-1}$ and CO₂/CH₄ selectivity of 12.9.⁶² Marti et al. prepared a ZIF-8 membrane with CO₂ permeance of $0.7 \times 10^{-8} \text{ mol m}^{-2} \text{ s}^{-1} \text{ Pa}^{-1}$ and CO₂/N₂ selectivity of 52.⁶³ Lin et al. found that the MOF-5 membrane exhibited extremely high selectivity of 410 for the

CO₂/N₂ mixture with CO₂ concentration of 87.4%. However, the separation performance for the feed gases with lower CO₂ concentration was poor.¹⁸ In comparison, the PDA/UiO-66 membrane had competitive separation performance and good balance between permeance and selectivity. Because of the small thickness, intact interior pore structure, preferential CO₂ adsorption and suppressed noneffective passageways, the PDA/UiO-66 membrane possessed 2–3 times higher selectivity than the reported MOF membranes with similar permeance, or 2–3 orders of magnitude larger permeance than those membranes with similar selectivity (SI Tables S4 and S5).

Separation Mechanism. The separation of MOF membranes is controlled by the affinities of selective layers to gas molecules and the apertures of frameworks. The gas sorption of MOFs and the gas diffusion in membranes are vital for separation performance. UiO-66 framework has apertures of 0.6 nm,⁶⁴ which is bigger than the kinetic diameters of the tested gases. We investigated the porous structures of UiO-66 particles collected from the bulk solution after membrane synthesis by nitrogen adsorption–desorption isotherms (SI Figure S7). The UiO-66 particles had high BET specific surface area of 1332.3 m² g⁻¹ (Figure 8a). The pore width distribution indicated that the UiO-66 possessed mainly apertures of 0.6 and 1.2 nm, which were consistent with the reports in previous study.⁵⁰ The adsorption properties of UiO-66 to CO₂, CH₄ and N₂ were studied as well (Figure 8b). Because Zr₆O₄(OH)₄ clusters had specific interaction with CO₂, the UiO-66 particles showed much greater CO₂ adsorption capability than other two gases. The adsorption capacity was ordered by CO₂, CH₄ and N₂, which agreed with that of the gas permeance. The permeability (*P*) is related to sorption coefficient (*S*) and diffusion coefficient (*D*) through

the equation of $P = D \times S$.⁴⁰ S can be derived from the adsorption isotherms and crystalline density of UiO-66.^{65,66} D can be back-calculated by $D = P/S$. As shown in SI Table S6, the UiO-66 had excellent CO₂/CH₄ and CO₂/N₂ sorption selectivities. Those results proved that the UiO-66 membrane was mainly governed by preferential adsorption.

After PDA postmodification, the permeance of PDA/UiO-66 membrane decreased slightly but selectivity increased greatly. In order to investigate whether the dopamine can be impregnated into pore structures of UiO-66 frameworks, we studied the porosity of PDA/UiO-66 particles (Figure 8c). The specific surface area of 1345.4 m² g⁻¹ and pore width distribution with peaks at 0.6 and 1.2 nm were similar to those of the UiO-66 particles. These results confirmed that the ultrathin PDA was only deposited on the surface and UiO-66 maintained the intact porous structures after postmodification. The intact interior pore structures combined with the thin selective layer resulted in the high permeance of the PDA/UiO-66 membrane. Figure 8d shows the gas adsorption properties of the PDA/UiO-66 particles. Because the amount of the coated PDA was low, the adsorption capacity only displayed a small change after modification. This revealed that the main adsorbents were frameworks for both UiO-66 and PDA/UiO-66. After modification, the simultaneously increased CO₂, CH₄ and N₂ sorption coefficients brought about the slightly decreased sorption selectivities (SI Table S6). However, similar reduction by 4–5 × 10⁻⁸ cm² s⁻¹ in diffusion coefficients of three gases in membranes caused the significant enhancement in CO₂/CH₄ and CO₂/N₂ diffusion selectivities, since the CO₂ diffusion coefficient was remarkably greater than that of CH₄ and N₂ (SI Table S6). The improvement in diffusion selectivity was the main factor for the better separation performance of the PDA/UiO-66 membrane than that of the original one. We speculated the enhancement in diffusion selectivity of the PDA/UiO-66 membrane as follow. For MOF membranes, there were often some unobservable nanometer-sized pinholes and grain boundaries, which offered the invalid channels for nonselective gas transports.^{41,44} On account of the similar amount in reduction of CO₂, CH₄ and N₂ diffusion coefficients and the intact interior pore structures of the PDA/UiO-66, the PDA impregnation in invalid pinholes and grain boundaries for suppressing the nonselective permeation was considered as the dominant factor for the improved selectivity. As well as the tailoring of PDA polymer chains to the exposed pores of membrane surface might also contribute to the enhancement in selectivity.

In summary, we have demonstrated that the versatile PDA postmodification can greatly improve CO₂ capture performance of MOF membranes. PDA with strong bioadhesion can be simply grafted on the UiO-66 membrane under mild conditions. The postmodified PDA/UiO-66 membrane exhibits impressive CO₂ permeance and selectivities in CO₂/N₂ and CO₂/CH₄ separations, because PDA blocks off the invalid pinholes and grain boundaries but do not change the pore structures of frameworks. The CO₂ capture performance surpasses the trade-off limitation of polymeric membranes easily. The PDA/UiO-66 membrane displays good reproducibility and excellent long-term stability as well. The simple and efficient modification processes, coupled with the competitive performance, present that PDA postmodification of MOF membranes reported here provides an alternative route for obtaining CO₂ capture separation membranes. Although the preparation cost of MOF membranes are relative high,

regarding the excellent separation performance, we humbly believe the investigations of MOF membranes just the beginning to future prosperity.

■ ASSOCIATED CONTENT

Supporting Information

The Supporting Information is available free of charge on the ACS Publications website at DOI: 10.1021/acs.est.9b00408.

Characterizations (SEM, FTIR, and XRD) and separation performance of the PDA/UiO-66 membrane, and comparison of gas separation performance (PDF)

■ AUTHOR INFORMATION

Corresponding Author

*E-mail: gandylin@126.com.

ORCID

Wanbin Li: 0000-0003-2460-168X

Author Contributions

W.L. conceived the research idea and formulated the project. W.W., Z. L., and W.L. performed the fabrication and characterization of UiO-66 particles and membranes. W.W., Y.C., and W.L. carried out the experiments of gas permeation and separation. W.W. and W.L. wrote the paper. All authors contributed to the revising the paper.

Notes

The authors declare no competing financial interest.

■ ACKNOWLEDGMENTS

This work was financially supported by the National Natural Science Foundation of China (Grant No. 51708252), the Fundamental Research Funds for the Central Universities (Grant No. 21617322), and Jinan University (Grant No. 88016674).

■ REFERENCES

- (1) Fuglestad, J.; Berntsen, T.; Eyring, V.; Isaksen, I.; Lee, D. S.; Sausen, R. Shipping Emissions: From Cooling to Warming of Climate and Reducing Impacts on Health. *Environ. Sci. Technol.* **2009**, *43*, 9057–9062.
- (2) Qu, S.; Li, Y.; Liang, S.; Yuan, J.; Xu, M. Virtual CO₂ Emission Flows in the Global Electricity Trade Network. *Environ. Sci. Technol.* **2018**, *52*, 6666–6675.
- (3) Li, P.; Zeng, H. C. Hierarchical Nanocomposite by the Integration of Reduced Graphene Oxide and Amorphous Carbon with Ultrafine MgO Nanocrystallites for Enhanced CO₂ Capture. *Environ. Sci. Technol.* **2017**, *51*, 12998–13007.
- (4) Wang, S.; Li, X.; Wu, H.; Tian, Z.; Xin, Q.; He, G.; Peng, D.; Chen, S.; Yin, Y.; Jiang, Z.; Guiver, M. D. Advances in High Permeability Polymer-Based Membrane Materials for CO₂ Separations. *Energy Environ. Sci.* **2016**, *9*, 1863–1890.
- (5) Seoane, B.; Coronas, J.; Gascon, I.; Etxebarria Benavides, M.; Karvan, O.; Caro, J.; Kapteijn, F.; Gascon, J. Metal-Organic Framework Based Mixed Matrix Membranes: a Solution for Highly Efficient CO₂ Capture? *Chem. Soc. Rev.* **2015**, *44*, 2421–2454.
- (6) Zhang, S.; Shen, Y.; Shao, P.; Chen, J.; Wang, L. Kinetics, Thermodynamics, and Mechanism of a Novel Biphasic Solvent for CO₂ Capture from Flue Gas. *Environ. Sci. Technol.* **2018**, *52*, 3660–3668.
- (7) Anjum, M. W.; Vermoortele, F.; Khan, A. L.; Bueken, B.; De Vos, D. E.; Vankelecom, I. F. Modulated UiO-66-Based Mixed-Matrix Membranes for CO₂ Separation. *ACS Appl. Mater. Interfaces* **2015**, *7*, 25193–25201.
- (8) Yuan, M.; Liguori, S.; Lee, K.; Van Campen, D. G.; Toney, M. F.; Wilcox, J. Vanadium As a Potential Membrane Material for

Carbon Capture: Effects of Minor Flue Gas Species. *Environ. Sci. Technol.* **2017**, *51*, 11459–11467.

(9) Zhai, H.; Rubin, E. S. Systems Analysis of Physical Absorption of CO₂ in Ionic Liquids for Pre-Combustion Carbon Capture. *Environ. Sci. Technol.* **2018**, *52*, 4996–5004.

(10) Baker, R. W.; Low, B. T. Gas Separation Membrane Materials: A Perspective. *Macromolecules* **2014**, *47*, 6999–7013.

(11) Ghalei, B.; Sakurai, K.; Kinoshita, Y.; Wakimoto, K.; Isfahani, A. P.; Song, Q. L.; Doitomi, K.; Furukawa, S.; Hirao, H.; Kusuda, H.; Kitagawa, S.; Sivaniah, E. Enhanced Selectivity in Mixed Matrix Membranes for CO₂ Capture through Efficient Dispersion of Amine-Functionalized MOF Nanoparticles. *Nat. Energy* **2017**, *2*, 17086.

(12) Merkel, T. C.; Lin, H.; Wei, X.; Baker, R. Power Plant Post-Combustion Carbon Dioxide Capture: An Opportunity for Membranes. *J. Membr. Sci.* **2010**, *359*, 126–139.

(13) Dechnik, J.; Gascon, J.; Doonan, C. J.; Janiak, C.; Sumbly, C. J. Mixed-Matrix Membranes. *Angew. Chem., Int. Ed.* **2017**, *56*, 9292–9310.

(14) Wang, T.; Zhao, L.; Shen, J.; Wu, L.; Bruggen, B. V. Enhanced Performance of Polyurethane Hybrid Membranes for CO₂ Separation by Incorporating Graphene Oxide: The Relationship between Membrane Performance and Morphology of Graphene Oxide. *Environ. Sci. Technol.* **2015**, *49*, 8004–8011.

(15) Sabetghadam, A.; Seoane, B.; Keskin, D.; Duim, N.; Rodenas, T.; Shahid, S.; Sorribas, S.; Le Guillouzer, C.; Clet, G.; Tellez, C.; Daturi, M.; Coronas, J.; Kapteijn, F.; Gascon, J. Metal Organic Framework Crystals in Mixed-Matrix Membranes: Impact of the Filler Morphology on the Gas Separation Performance. *Adv. Funct. Mater.* **2016**, *26*, 3154–3163.

(16) Wang, T.; Cheng, C.; Wu, L.; Shen, J.; Bruggen, B. V.; Chen, Q.; Chen, D.; Dong, C. Fabrication of Polyimide Membrane Incorporated with Functional Graphene Oxide for CO₂ Separation: The Effects of GO Surface Modification on Membrane Performance. *Environ. Sci. Technol.* **2017**, *51*, 6202–6210.

(17) Friebe, S.; Geppert, B.; Steinbach, F.; Caro, J. Metal-Organic Framework UiO-66 Layer: A Highly Oriented Membrane with Good Selectivity and Hydrogen Permeance. *ACS Appl. Mater. Interfaces* **2017**, *9*, 12878–12885.

(18) Rui, Z.; James, J. B.; Kasik, A.; Lin, Y. S. Metal-organic Framework Membrane Process for High Purity CO₂ Production. *AIChE J.* **2016**, *62*, 3836–3841.

(19) Qiu, S.; Xue, M.; Zhu, G. Metal-organic Framework Membranes: From Synthesis to Separation Application. *Chem. Soc. Rev.* **2014**, *43*, 6116–6140.

(20) Li, W.; Zhang, G.; Zhang, C.; Meng, Q.; Fan, Z.; Gao, C. Synthesis of Trinity Metal-Organic Framework Membranes for CO₂ Capture. *Chem. Commun.* **2014**, *50*, 3214–3216.

(21) Zhou, F.; Tien, H. N.; Xu, W. L.; Chen, J. T.; Liu, Q.; Hicks, E.; Fathizadeh, M.; Li, S.; Yu, M. Ultrathin Graphene Oxide-Based Hollow Fiber Membranes with Brush-Like CO₂-Philic Agent for Highly Efficient CO₂ Capture. *Nat. Commun.* **2017**, *8*, 2107.

(22) Hong, S.; Kim, D.; Jeong, Y.; Kim, E.; Jung, J. C.; Choi, N.; Nam, J.; Yip, A. C. K.; Choi, J. Healing of Microdefects in SSZ-13 Membranes via Filling with Dye Molecules and Its Effect on Dry and Wet CO₂ Separations. *Chem. Mater.* **2018**, *30*, 3346–3358.

(23) Robeson, L. M. The Upper Bound Revisited. *J. Membr. Sci.* **2008**, *320*, 390–400.

(24) Li, W. Metal-Organic Framework Membranes: Production, Modification, and Applications. *Prog. Mater. Sci.* **2019**, *100*, 21–63.

(25) Liu, Y.; Ban, Y.; Yang, W. Microstructural Engineering and Architectural Design of Metal-Organic Framework Membranes. *Adv. Mater.* **2017**, *29*, 1606949.

(26) Li, W.; Su, P.; Li, Z.; Xu, Z.; Wang, F.; Ou, H.; Zhang, J.; Zhang, G.; Zeng, E. Ultrathin Metal-organic Framework Membrane Production by Gel-Vapour Deposition. *Nat. Commun.* **2017**, *8*, 406.

(27) Hurtle, S.; Friebe, S.; Wohlgemuth, J.; Woll, C.; Caro, J.; Heinke, L. Sprayable, Large-Area Metal-Organic Framework Films and Membranes of Varying Thickness. *Chem. - Eur. J.* **2017**, *23*, 2294–2298.

(28) Li, W.; Yang, Z.; Zhang, G.; Fan, Z.; Meng, Q.; Shen, C.; Gao, C. Stiff Metal-Organic Framework-Polyacrylonitrile Hollow Fiber Composite Membranes with High Gas Permeability. *J. Mater. Chem. A* **2014**, *2*, 2110–2118.

(29) Zhang, F.; Zo, X.; Gao, X.; Fan, S.; Sun, F.; Ren, H.; Zhu, G. Hydrogen Selective NH₂-MIL-53(Al) MOF Membranes with High Permeability. *Adv. Funct. Mater.* **2012**, *22*, 3583–3590.

(30) Li, W.; Su, P.; Zhang, G.; Shen, C.; Meng, Q. Preparation of Continuous NH₂-MIL-53 Membrane on Ammoniated Polyvinylidene Fluoride Hollow Fiber for Efficient H₂ Purification. *J. Membr. Sci.* **2015**, *495*, 384–391.

(31) Pan, Y. C.; Li, T.; Lestari, G.; Lai, Z. P. Effective Separation of Propylene/Propane Binary Mixtures by ZIF-8 Membranes. *J. Membr. Sci.* **2012**, *390*, 93–98.

(32) Brown, A. J.; Brunelli, N. A.; Eum, K.; Rashidi, F.; Johnson, J. R.; Koros, W. J.; Jones, C. W.; Nair, S. Interfacial Microfluidic Processing of Metal-Organic Framework Hollow Fiber Membranes. *Science* **2014**, *345*, 72–75.

(33) Barankova, E.; Tan, X.; Villalobos, L. F.; Litwiller, E.; Peinemann, K. V. A Metal Chelating Porous Polymeric Support: The Missing Link for a Defect-Free Metal-Organic Framework Composite Membrane. *Angew. Chem., Int. Ed.* **2017**, *56*, 2965–2968.

(34) Ma, X.; Kumar, P.; Mittal, N.; Khlyustova, A.; Daoutidis, P.; Mkhoyan, K. A.; Tsapatsis, M. Zeolitic Imidazolate Framework Membranes Made by Ligand-Induced Permselectivation. *Science* **2018**, *361*, 1008–1011.

(35) Yin, H.; Wang, J.; Xie, Z.; Yang, J.; Bai, J.; Lu, J.; Zhang, Y.; Yin, D.; Lin, J. Y. A Highly Permeable and Selective Amino-Functionalized MOF CAU-1 Membrane for CO₂-N₂ Separation. *Chem. Commun.* **2014**, *50*, 3699–3701.

(36) Cacho-Bailo, F.; Caro, J.; Etxeberria-Benavides, M.; Karvan, O.; Tellez, C.; Coronas, J. High Selectivity ZIF-93 Hollow Fiber Membranes for Gas Separation. *Chem. Commun.* **2015**, *51*, 11283–11285.

(37) Cacho-Bailo, F.; Etxeberria-Benavides, M.; Karvan, O.; Téllez, C.; Coronas, J. Sequential Amine Functionalization Inducing Structural Transition in an Aldehyde-Containing Zeolitic Imidazolate Framework: Application to Gas Separation Membranes. *CrystEngComm* **2017**, *19*, 1545–1554.

(38) Xie, K.; Fu, Q.; Xu, C.; Lu, H.; Zhao, Q.; Curtain, R.; Gu, D.; Wibley, P. A.; Qiao, G. G. Continuous Assembly of a Polymer on a Metal-Organic Framework (CAP on MOF): a 30 nm Thick Polymeric Gas Separation Membrane. *Energy Environ. Sci.* **2018**, *11*, 544–550.

(39) Cohen, S. M. Postsynthetic Methods for the Functionalization of Metal-Organic Frameworks. *Chem. Rev.* **2012**, *112*, 970–1000.

(40) Koros, W. J.; Zhang, C. Materials for Next-Generation Molecularly Selective Synthetic Membranes. *Nat. Mater.* **2017**, *16*, 289–297.

(41) Huang, A.; Caro, J. Covalent Post-Functionalization of Zeolitic Imidazolate Framework ZIF-90 Membrane for Enhanced Hydrogen Selectivity. *Angew. Chem., Int. Ed.* **2011**, *50*, 4979–4982.

(42) Hong, M.; Falconer, J. L.; Noble, R. D. Modification of Zeolite Membranes for H₂ Separation by Catalytic Cracking of Methyl-diethoxysilane. *Ind. Eng. Chem. Res.* **2005**, *44*, 4035–4041.

(43) Yoo, Y.; Varela-Guerrero, V.; Jeong, H. K. Isorecticular Metal-Organic Frameworks and Their Membranes with Enhanced Crack Resistance and Moisture Stability by Surfactant-assisted Drying. *Langmuir* **2011**, *27*, 2652–2657.

(44) Huang, A.; Wang, N.; Kong, C.; Caro, J. Organosilica-Functionalized Zeolitic Imidazolate Framework ZIF-90 Membrane with High Gas-Separation Performance. *Angew. Chem., Int. Ed.* **2012**, *51*, 10551–10555.

(45) Lee, M. J.; Kwon, H. T.; Jeong, H. K. High-Flux Zeolitic Imidazolate Framework Membranes for Propylene/Propane Separation by Postsynthetic Linker Exchange. *Angew. Chem., Int. Ed.* **2018**, *57*, 156–161.

(46) Sun, D. T.; Peng, L.; Reeder, W. S.; Moosavi, S. M.; Tiana, D.; Britt, D. K.; Oveisi, E.; Queen, W. L. Rapid, Selective Heavy Metal

Removal from Water by a Metal-Organic Framework/Polydopamine Composite. *ACS Cent. Sci.* **2018**, *4*, 349–356.

(47) Yang, H. C.; Luo, J.; Lv, Y.; Shen, P.; Xu, Z. K. Surface Engineering of Polymer Membranes via Mussel-Inspired Chemistry. *J. Membr. Sci.* **2015**, *483*, 42–59.

(48) Hong, S.; Na, Y. S.; Choi, S.; Song, I. T.; Kim, W. Y.; Lee, H. Non-Covalent Self-Assembly and Covalent Polymerization Co-Contribute to Polydopamine Formation. *Adv. Funct. Mater.* **2012**, *22*, 4711–4717.

(49) Cavka, J. H.; Jakobsen, S.; Olsbye, U.; Guillou, N.; Lamberti, C.; Bordiga, S.; Lillerud, K. P. A New Zirconium Inorganic Building Brick Forming Metal Organic Frameworks with Exceptional Stability. *J. Am. Chem. Soc.* **2008**, *130*, 13850–13851.

(50) Wu, H.; Chua, Y. S.; Krungleviciute, V.; Tyagi, M.; Chen, P.; Yildirim, T.; Zhou, W. Unusual and Highly Tunable Missing-Linker Defects in Zirconium Metal-Organic Framework UiO-66 and Their Important Effects on Gas Adsorption. *J. Am. Chem. Soc.* **2013**, *135*, 10525–10532.

(51) Cmarik, G. E.; Kim, M.; Cohen, S. M.; Walton, K. S. Tuning the Adsorption Properties of UiO-66 via Ligand Functionalization. *Langmuir* **2012**, *28*, 15606–15613.

(52) Shearer, G. C.; Chavan, S.; Bordiga, S.; Svelle, S.; Olsbye, U.; Lillerud, K. P. Defect Engineering: Tuning the Porosity and Composition of the Metal-Organic Framework UiO-66 via Modulated Synthesis. *Chem. Mater.* **2016**, *28*, 3749–3761.

(53) Kwon, H. T.; Jeong, H. K. In Situ Synthesis of Thin Zeolitic-Imidazolate Framework ZIF-8 Membranes Exhibiting Exceptionally High Propylene/Propane Separation. *J. Am. Chem. Soc.* **2013**, *135*, 10763–10768.

(54) Liu, Q.; Wang, N.; Caro, J.; Huang, A. Bio-Inspired Polydopamine: A Versatile and Powerful Platform for Covalent Synthesis of Molecular Sieve Membranes. *J. Am. Chem. Soc.* **2013**, *135*, 17679–17682.

(55) Karan, S.; Jiang, Z.; Livingston, A. G. Sub-10nm Polyamide Nanofilms with Ultrafast Solvent Transport for Molecular Separation. *Science* **2015**, *348*, 1347–1351.

(56) Li, H.; Song, Z. N.; Zhang, X. J.; Huang, Y.; Li, S. G.; Mao, Y. T.; Ploehn, H. J.; Bao, Y.; Yu, M. Ultrathin, Molecular-Sieving Graphene Oxide Membranes for Selective Hydrogen Separation. *Science* **2013**, *342*, 95–98.

(57) Rodrigues, M. A.; Ribeiro, J. d. S.; Costa, E. d. S.; Miranda, J. L. d.; Ferraz, H. C. Nanostructured Membranes Containing UiO-66 (Zr) and MIL-101 (Cr) for O₂/N₂ and CO₂/N₂ separation. *Sep. Purif. Technol.* **2018**, *192*, 491–500.

(58) Dong, L.; Chen, M.; Wu, X.; Shi, D.; Dong, W.; Zhang, H.; Zhang, C. Multi-Functional Polydopamine Coating: Simultaneous Enhancement of Interfacial Adhesion and CO₂ Separation Performance of Mixed Matrix Membranes. *New J. Chem.* **2016**, *40*, 9148–9159.

(59) Liu, X.; Demir, N. K.; Wu, Z.; Li, K. Highly Water-Stable Zirconium Metal-Organic Framework UiO-66 Membranes Supported on Alumina Hollow Fibers for Desalination. *J. Am. Chem. Soc.* **2015**, *137*, 6999–7002.

(60) Venna, S. R.; Carreon, M. A. Highly Permeable Zeolite Imidazolate Framework-8 Membranes for CO₂/CH₄ Separation. *J. Am. Chem. Soc.* **2010**, *132*, 76–8.

(61) Yin, H.; Wang, J.; Xie, Z.; Yang, J.; Bai, J.; Lu, J.; Zhang, Y.; Yin, D.; Lin, J. Y. S. Highly Permeable and Selective Amino-Functionalized MOF CAU-1 Membrane for CO₂/N₂ Separation. *Chem. Commun.* **2014**, *50*, 3699–3701.

(62) Liu, Y.; Pan, J. H.; Wang, N.; Steinbach, F.; Liu, X.; Caro, J. Remarkably Enhanced Gas Separation by Partial Self-Conversion of a Laminated Membrane to Metal-Organic Frameworks. *Angew. Chem., Int. Ed.* **2015**, *54*, 3028–3032.

(63) Marti, A. M.; Wickramanayake, W.; Dahe, G.; Sekizkardes, A.; Bank, T. L.; Hopkinson, D. P.; Venna, S. R. Continuous Flow Processing of ZIF-8 Membranes on Polymeric Porous Hollow Fiber Supports for CO₂ Capture. *ACS Appl. Mater. Interfaces* **2017**, *9*, 5678–5682.

(64) Shen, J.; Liu, G.; Huang, K.; Li, Q.; Guan, K.; Li, Y.; Jin, W. UiO-66-Polyether Block Amide Mixed Matrix Membranes for CO₂ Separation. *J. Membr. Sci.* **2016**, *513*, 155–165.

(65) Al-Maythaly, B. A.; Shekha, O.; Swaidan, R.; Belmabkhout, Y.; Pinnau, I.; Eddaoudi, M. Quest for Anionic MOF Membranes: Continuous sod-ZMOF Membrane with CO₂ Adsorption-Driven Selectivity. *J. Am. Chem. Soc.* **2015**, *137*, 1754–1757.

(66) Guillerm, V.; Ragon, F.; Dan-Hardi, M.; Devic, T.; Vishnuvarthan, M.; Campo, B.; Vimont, A.; Clet, G.; Yang, Q.; Maurin, G.; Férey, G.; Vittadini, A.; Gross, S.; Serre, C. A Series of Isorecticular, Highly Stable, Porous Zirconium Oxide Based Metal-Organic Frameworks. *Angew. Chem., Int. Ed.* **2012**, *51*, 9267–9271.